AINTEGUMENTA homolog expression in Gnetum (gymnosperms) and implications for the evolution of ovulate axes in seed plants

AINTEGUMENTA homologue expression in *Gnetum* (gymnosperms) and implications for the evolution of ovulate axes in seed plants

Running title -- *ANT* homologue expression in *Gnetum*

Toshihiro Yamada [a], *, Yumiko Hirayama [b], Ryoko Imaichi [c], and Masahiro Kato [b]

[a] Division of Life Sciences, Graduate School of Natural Science and Technology, Kanazawa University, Kanazawa 920-1192, Japan (Phone and Fax: +81-76-264-6207)

[b] Department of Botany, National Museum of Nature and Science, Amakubo, Tsukuba 305-0005, Japan (Phone and Fax:

+81-29-853-8970)

^c Department of Chemical and Biological Sciences, Japan Women's

University, Mejirodai, Tokyo 112-8681, Japan   (Phone and Fax:

+81-3-5981-3662)

[*] Author for correspondence (email: ptilo@mb.infoweb.ne.jp)

Authors' current addresses are the same as those at the time the work

was conducted.

Word count for manuscript: 5209

SUMMARY The expression of *GpANTL1*, a homolog of

AINTEGUMENTA (*ANT*) found in the gymnosperm *Gnetum parvifolium*,

was analyzed by RT-PCR and *in situ* hybridization. *GpANTL1* was

expressed in the leaf primordia, root tips, and young ovules. In the

ovulate axis, expression was detected as four distinct rings around the

outer, middle, and inner envelope primordia as well as around the

nucellar tip. This pattern of expression is similar to that of *ANT* in

Arabidopsis thaliana. A comparison of the expression of *GpANTL1* with

that of *PtANTL1* in the conifer *Pinus thunbergii* suggests that the

integrated expression of *PtANTL1* may have been caused by congenital

fusion of the integument, ovuliferous scale, and bract.

INTRODUCTION

Since the origin of the ovule in the Devonian period (Stewart and

Rothwell 1993), the morphology of the distal–proximal ovulate axis has

diversified in seed plants (Florin 1951; Crane 1985; Doyle and

Donoghue 1986). The nearly sessile gymnosperm ovule is composed of

a distal nucellus, which harbors the female gametophyte with several

archegonia and a proximal integument. The integument surrounds the

nucellus completely except for a small opening known as the micropyle.

The micropyle is at the distal end of the ovule, opposite the proximal

connection to the sporophyll, resulting in an orthotropous configuration

(Coulter and Chamberlain 1917; Bouman 1984; Gifford and Foster 1988).

In some extant gymnosperm lineages, such as the Gnetales and

Coniferales, the ovule is enveloped by a single integument (i.e., a

unitegmic ovule), and this structure is incorporated with the shoot and

lateral organs (i.e., the sporophylls and bract) into a complicated ovulate

axis. In contrast, in the Cycadales, the ovules are simply borne on the

megasporophyll, while in the Ginkgoales, pairs of ovules terminate on a stalk (Coulter and Chamberlain 1917; Florin 1951; Crane 1985; Doyle and Donoghue 1986; Gifford and Foster 1988; Shindo et al. 1999).

The angiosperm ovulate axis is characterized by an acropetal sequence that includes the funiculus, which connects the ovule to the placenta, outer and inner integuments that flank the chalaza, and the nucellus around the embryo sac (Bouman 1984; Robinson-Beers et al. 1992). The micropyle, which is formed either by both integuments or by only the inner integument, sits adjacent to the funiculus in anatropous ovules, or opposite in orthotropous ovules. Developmental similarities suggest homology between the inner integument of the angiosperms and the lone integument of the gymnosperms (Bouman 1984; Umeda et al. 1994), while the outer integument is inferred to be homologous to a leaflike organ (Umeda et al. 1994; Imaichi et al. 1995; Meister et al. 2003; Yamada et al. 2001a, b, 2003). Thus, in angiosperms, the unitegmic ovule and a leaflike organ should be integrated into the ovulate axis.

To determine what evolutionary changes gave rise to the

complicated ovulate axis of seed plants, it is necessary to evaluate the genetic basis of ovulate axis formation among extant seed plants.

AINTEGUMENTA (*ANT*), a member of the AP2 subfamily within the AP2/ERBP family, is involved in ovule development in *Arabidopsis thaliana* and required for proper integument growth (Elliott et al. 1996; Klucher et al. 1996; Mizukami and Fischer 2000; Shigyo and Ito 2004; Kim et al. 2006; Shigyo et al. 2006). *ANT* is transcribed throughout the ovule primordia during Stage 8, when the primordia emerge from the placenta (Elliot et al. 1996; Klucher et al. 1996; Schneitz 1998; Balasubramanian and Schneitz 2000, 2002; Seiber et al. 2004). During Stages 9 and 10, *ANT* expression is negatively regulated in the nucellus and funiculus by *NOZZLE/SPOROCYTRLESS* (*NZZ/SPL*), resulting in restricted expression in the chalaza (i.e., where the inner and outer integuments will be formed) (Elliot et al. 1996; Klucher et al. 1996; Schneitz 1998; Balasubramanian and Schneitz 2000, 2002; Seiber et al. 2004). Previously, a gymnospermous *ANT* homolog was isolated from *Pinus thunbergii* Parl. (Pinaceae, Coniferales) and its expression was analyzed by *in situ* hybridization and RT-PCR (Shigyo and Ito 2004).

However, due to its highly modified nature (e.g., Florin 1951; Gifford and Foster 1988), the ovulate axis in the Coniferales is difficult to compare with the ovulate axis of the angiosperms. Gnetales is the putative sister of the Pinaceae or Coniferales among the extant gymnosperms (Winter et al. 1999; Soltis et al. 2002; Burleigh and Mathews 2004), but its members have a less complex ovulate axis than the Coniferales (Coulter and Chamberlain 1917; Florin 1951; Crane 1985; Gifford and Foster 1988; Shindo et al. 1999). Thus, the expression of an *ANT* homolog in the Gnetales would not only help explain the genetic basis underlying the differences between the ovules of gymnosperms and angiosperms, but it would also help elucidate the evolutionary process that led to the modified ovulate structure of the Coniferales.

As well as the role that *ANT* played in the ovule evolution, its significant developmental role roused much interests to the evolution of *ANT* homologs (Shigyo and Ito, 2004; Kim et al. 2006; Shigyo et al. 2006; Floyd and Bowman, 2007). *ANT* is believed to regulate cellular proliferation via maintenance of the meristematic competence of other lateral organs (i.e., on the vegetative and reproductive axes), such as

the leaves, floral organs and integuments in *A. thaliana* (Mizukami and Fischer 2000). However, a little data is available on the function and expression of *ANT* homologs in other species than *A. thaliana*, hindering the inference of their evolution.

In this study, we analyzed the expression of *GpANTL1*, an *ANT* homolog in *Gnetum parvifolium* (Warb.) C. Y. Cheng (Shigyo et al. 2006), by RT-PCR and *in situ* hybridization. We then compared our data with that of *ANT* in *A. thaliana* (Elliot et al. 1996; Klucher et al. 1996; Schneitz 1998; Balasubramanian and Schneitz 2000, 2002) and inferred the ancestral function of *ANT* homologs. Furthermore, we compared the expression of *GpANTL1* in ovulate axis to that of *ANT* in ovule of *A. thaliana* as well as that of *PtANTL1* in the reproductive shoots of *P. thunbergii* (Shigyo and Ito 2004). The implications of our data for the evolution of the ovulate axis in seed plants is also discussed.

MATERIALS AND METHODS

Plant materials

Female strobili of *G. parvifolium* were collected from a plant cultivated in

the Botanical Gardens, Graduate School of Science, University of Tokyo,

from May to June 2006, and the ovules were dissected from the strobili

on ice. Leaf primordia, root tips, and vegetative shoots were collected

from a single plant of *G. parvifolium* in August and December 2007. This

plant was also used for the isolation of *GpAP2L1* and *GpANTL1* by

Shigyo et al. (2006).

All tissues were frozen in liquid nitrogen for use in the isolation of

GpANTL1 and RT-PCR analysis. For *in situ* hybridization, female strobili

and vegetative shoots were fixed in 4% formaldehyde (w/v) in which the

pH had been adjusted to 7.0 with NaP_i buffer for 15 h. In female strobili,

the collenchymatous tissue of the annular collar was removed to

facilitate fixation.

Isolation of *GpANTL1*

Total nucleic acids were extracted from the ovules with cethy trimethyl

ammonium bromide（CTAB) (Doyle and Doyle 1987) and then applied to

an RNeasy mini column (QIAGEN, Hilden, Germany) from an RNeasy

Mini Kit (QIAGEN) to obtain total RNA. Single-stranded cDNA was

subsequently synthesized using the 3' RACE System for Rapid

Amplification of cDNA Ends (Invitrogen, Carlsbad, CA, USA) according

to the manufacturer's protocol. Two gene-specific primers, GpANTF1

(5'-CACAAGGCACAGATGGACAG-3') and GpANTF2 (5'-

GGCTCATTTGTGGGACAACA-3'), were designed based on partial

sequences of *GpANTL1* (AB195247) registered in the DDBJ/EMBL/NCBI

database, and nested PCR was conducted using the amplified product.

GpANTF1 and Universal Amplification Primer (UAP) (Invitrogen) were

used in the first round of PCR, while GpANTF2 and UAP were used for

the nested PCR. Three internal primers for 5' RACE were subsequently

designed based on the sequences obtained from the 3' RACE

amplification: GpANT5R1 (5'- GCTTCATCTCATCAATCTGC-3'),

GpANTR2 (5'- GCCTTTTCCTCCTGATCGTA-3'), and GpANT5R3 (5'-

GCTCTGCCCTTCTTTTTTGC-3'). Amplification of the 5' partial cDNA

fragments was performed using the 5' RACE System for Rapid

Amplification of cDNA Ends (Invitrogen). The sequence of *GpANTL1*

(2005 bp) is registered as AB297493 in the DDBJ.

Alignment and phylogenetic analysis

Initially, the nucleotide sequences of *ANT* and several (outgroup) *AP2*

genes were retrieved from the DDBJ/EMBL/NCBI DNA database (S1).

Their amino acid sequences were then deduced and aligned using

CLUSTAL X, v. 1.83 (Thompson et al. 1997). The residues within the two

AP2 domains and the linker region between them were used for the

phylogenetic analyses.

Bayesian phylogenetic analysis was performed using BEAST v. 1.4

(Drummond and Rambaut 2006). The JTT + G model of amino acid

substitution, which assumes a gamma distribution to accommodate for

the rate of variation among sites, was adopted for the analysis because

the Akaike Information Criterion (AIC), the correlated AIC, and the

likelihoods calculated by ProtTest v. 1.2.6 (Abascal et al. 2005) all

predicted it as the best model of molecular evolution. The starting tree

for the Markov chain Monte Carlo (MCMC) analysis was generated using

a coalescent process. The trees were sampled every 1,000 steps for

10,000,000 steps after discarding 1,000,000 burn-in steps.

Convergence of the chain was verified using Tracer v. 1.3 (Rambaut and

Drummond 2005).

Maximum parsimony (MP) and bootstrap analyses were

implemented by PAUP*4.0b10 (Swofford 2001) using a heuristic search

strategy with 100 random addition sequence replicates and the TBR

branch-swapping algorithm. All optimal trees were saved in our MP

analyses, while ten trees per replicate of 1,000 total replicates were

saved in our bootstrap analyses.

Neighbor Joining (NJ) analysis was conducted using PHYLIP v.

3.56 (Felsenstain 1994). The distance matrix was generated using the

JTT matrix model of PROTDIST (Felsenstain 1994). A NJ tree was

generated using NEIGHBOR (Felsenstain 1994). Support for the clade

was evaluated by bootstrap analysis with 1,000 replicates.

RT-PCR

Total RNA was extracted from root tips, vegetative shoots, leaf primordia, young ovules, and developed ovules (i.e., those with three envelopes). RNA extraction and cDNA synthesis were performed as described for the isolation of *GpANTL1*.

Glyceraldehyde-3-phosphate dehydrogenase (*GAPDH*) was (AB362487 in the DDBJ) was amplified for normalization of the mRNA in the samples by PCR using the primers GpGAPF1 (5'-AAAGGTGTTACCTGCTCTTA-3') and GpGAPR1 (5'-CGTTCAGGGCTATGCCGGCC-3') (260-bp product). Partial *GpANTL1* cDNA was amplified using GpANTPF1 (5'-ACTGCCATCTGGCCACGTCG-3') and GpANTPR1 (5'-TGGGTGGCGTGGCTCAGGTG-3'). The amplified fragment included 410 bp just downstream of the AP2-repeat 2-domain coding region. A total of 30 cycles was used for the amplification of *GAPDH* and *GpANTL1*. The products were electrophoresed in a 1% agarose gel and stained with ethidium bromide.

In situ hybridization

The partial cDNA of *GpANTL1* was amplified by PCR using GpANTPF1 and GpANTPR1. The product was then cloned into pCR II (Invitrogen) and amplified using M13$^+$ (Invitrogen) and GpANTPR1 or M13$^-$ (Invitrogen) and GpANTPF1 for probe synthesis. Contaminating RNases were removed with RNAsecure Reagent (Ambion, Austin, TX, USA), and DIG-labeled antisense and sense riboprobes were synthesized as described previously (Yamada et al. 2003). *In situ* detection of *GpANTL1* transcription was performed as per Yamada et al. (2004).

RESULTS

ANT gene phylogeny

By Bayesian phylogenetic analysis, the monophyly of the *ANT* genes

was supported with a posterior probability of 100%. The *ANT* group

consisted of two clades, euANT and basalANT (*sensu* Kim et al. 2006),

each of which had a posterior probability of 100% (Fig. 1). Within the

euANT clade, two major clades, BBM/PLT and ANT (*sensu stricto*, *s.s.*),

were recognized with 99 and 100% posterior probabilities, respectively,

but the relationship between the two clades and *PpANT1* was not fully

resolved (Fig. 1). All gymnospermous *ANT* genes were nested in the

ANT (*s.s.*) clade, and formed a clade with a moderate posterior

probability value of 82% (gymnoANT clade in Fig. 1). However, all of the

angiosperm genes except *AIL1* were included in a single clade with a

posterior probability of 99%   (angioANT clade in Fig. 1). The

relationships among *AIL1*, the angioANT clade, and the gymnoANT

clade were not unambiguously supported (Fig. 1).

By both MP and NJ analyses, the ANT, basal ANT, euANT, and

BBM /PLT clades were recovered with more than 70% bootstrap support.

NJ analysis indicated monophyly for ANT (*s.s.*) including the gymnoANT

clade with 64% bootstrap support, but the ANT (*s.s.*) clade was not

recovered in a strict consensus tree by MP analysis.

GpANTL1 expression

GpANTL1 expression was detected in the vegetative shoots including

leaf primordia, leaf primordia, root tips, and young ovules. *GpANTL1*

expression was extremely weak in the developed ovules compared to

that in the young ovules (Fig. 2). In vegetative shoots, GpANTL1 was

expressed in leaf primordia. The stronger transcription is observed in

the abaxial and adaxial tissues of the leaf primordia, where the laminar

growth was taken place by active cell divisions (Fig. 3A, B).

Ovule formation was observed in the axil of the annular collar. Of

the three envelopes, the outer envelope developed first and covered the

ovulate axis long before the middle and inner envelope primordia

emerged. At this stage, *GpANTL1* expression was detected in the

abaxial epidermis and subdermis of the outer envelope as well as in the

inner and middle envelopes (Fig. 3C, D). It was also detected in the

nucellar tip (Fig. 3C, D). No signal was detected in the internode (i.e.,

between the inner and middle envelope anlagen) or in the tissues

between the middle and outer envelopes. Together, the regions where

GpANTL1 was expressed formed four separate rings around the ovulate

axis corresponding to the future nucellus and the outer, middle, and

inner envelopes (Figs. 3C, D). A little later, the middle envelope

emerged slightly, while the inner envelope primordium remained hidden

(Fig. 3E, F). As in the previous stage, *GpANTL1* expression was

detected in four distinct domains (the future nucellus and three

envelopes) (Figs. 3E, F). As the ovule developed further, the inner and

middle envelope primordia emerged (Fig. 3G, H). *GpANTL1* expression

was greatly diminished at this point in the outer and middle envelopes,

while some expression remained in the nucellar tip and inner envelope

(Fig. 3G, H).

DISCUSSION

Phylogeny of the *ANT* genes

The phylogenetic framework of the *ANT* genes included in this study is similar to those of previous studies in two respects: the group is subdivided into the basalANT and euANT clades, and the ANT (*s.s.*) and BBM/PLT clades are recovered within the euANT clade (Shigyo and Ito 2004; Kim et al. 2006; Shigyo et al. 2006; Floyd and Bowman 2007). As described earlier (Shigyo and Ito 2004; Shigyo et al. 2006; Floyd and Bowman 2007), all of the gymnosperm *ANT* genes reported so far are nested within the ANT (*s.s.*) clade. This implies that gene loss occurred at least once in the BBM/PLT and basalANT clades, or that genes related to these two lineages have not yet been isolated in gymnosperms.

Putative ancestral function of the ANT (*s.s.*) clade genes

In *Arabidopsis*, *ANT* is expressed in the developing lateral organs (i.e., on the vegetative and reproductive axes), such as the leaves, floral organs, and the inner and outer integuments (Elliott et al. 1996; Klucher et al. 1996; Krizek 1999; Mizukami and Fischer 2000). In the *ant* mutant,

organ size is reduced due to a decrease in cell number, while

constitutive *ANT* expression causes organ hyperplasia due to an

increase in cell number (Mizukami and Fischer 2000). Thus, *ANT* is

believed to regulate cellular proliferation via maintenance of the

meristematic competence of the lateral organs (Mizukami and Fischer

2000). Consistent with this idea, *ANT* expression in the lateral organs

decreases as organ development progresses (Elliott et al. 1996; Klucher

et al. 1996; Krizek 1999; Mizukami and Fischer 2000; Nole-Wilson et al.

2005). In addition to its expression in the lateral organs, *ANT* is also

expressed in the roots in *Arabidopsis*, although its function there is

unknown (Nole-Wilson et al. 2005). In gymnosperms, similar expression

of the *ANT* homolog *PtANTL1* was reported in the lateral organs of the

reproductive shoot in *P. thunbergii* (Pinaceae) (Fig. 4B; Shigyo and Ito

2004). However, no expression data are available for the leaf primordia

and roots, and thus the ancestral expression pattern and function of the

ANT (*s.s.*) genes are not well understood.

Developmental studies suggest that the inner envelope of *Gnetum*

is homologous to the integument (e.g., Takaso and Bouman 1986), while

the outer and middle envelopes are comparable to the leaves that

enclose unitegmic ovule(s) (Crane 1985; Shindo et al. 1999; Hasebe

1999). *GpANTL1* is expressed in the outer, middle, and inner envelopes

as well as in the leaf primordia and roots. This pattern is consistent with

that of *ANT* in *A. thaliana* (Elliott et al. 1996; Klucher et al. 1996; Krizek

1999; Mizukami and Fischer 2000; Nole-Wilson et al. 2005), suggesting

that this is the ancestral pattern of the ANT (*s.s.*) clade. Together, the

enhanced expression of *GpANTL1* in the young envelope primordia

versus that in the old primordia was observed in RT-PCR analysis and

its transcription is decreased in the differentiated tissues in the leaf

primordia. These data imply that regulation of cellular proliferation in the

lateral organs is the ancestral function of the *ANT* (*s.s.*) genes.

A major difference between *GpANTL1* and *ANT* is that *GpANTL1* is

expressed in the nucellar tip while *ANT* expression is absent from the

nucellus (Fig. 4A, C). Expression in the nucellar tip was previously

reported for *PtANTL1* in *P. thunbergii* (Fig. 4B; Shigyo and Ito 2004),

implying that it represents an ancestral pattern of gene expression in the

gymnospermous ovulate axis. Such divergent gene expression in

gymnosperms and angiosperms may be attributable to differential regulation of nucellar development or a remarkable change in the angiosperm nucellus.

Evolution of the ovulate axis in seed plants

The ANT (*s.s.*) clade genes are transcribed differently in *G. parvifolium* (Gnetales), *P. thunbergii* (Coniferales), and *A. thaliana* (angiosperms), but their expression is similar with respect to the lateral organs of the ovulate axis. *GpANTL1* is expressed separately in the developing inner, middle, and outer envelope primordia (Fig. 4A). In comparison, *PtANTL1* expression in *P. thunbergii* has been detected throughout the entire primordium of the bract and ovule–ovuliferous scale complex (Fig. 4B: Shigyo and Ito 2004). In contrast, in *A. thaliana*, *ANT* is expressed in a single band of cells including the chalaza and the developing inner and outer integument (Elliott et al. 1996; Klucher et al. 1996; Mizukami and Fischer 2000; Fig. 4C). How can this difference be interpreted from an evolutionary point of view?

It is widely accepted that two pairs of leaves fuse to create radially symmetrical outer and middle envelopes in the ancestral fertile shoot axis, which bears unitegmic ovules at its apical end (Crane 1985; Shindo et al. 1999), although no direct evidence is available. According to this interpretation, the ovulate axis of *Gnetum* is a highly contracted axis with three envelopes, each of which is a distinct developmental unit (Fig. 5A). The ovule-ovuliferous scale complex of the Coniferales is likely another highly condensed, modified fertile shoot subtended by the scaly bract (Florin 1951; Gifford and Foster 1988). Gene expression analyses supported this interpretation (Shindo et al. 1999; Hasebe 1999). Axis condensation may have caused lateral congenital fusion of the ovules and ovuliferous scale on the ovulate axis and subtending bract (Fig. 5B). The integrated expression of *PtANTL1* in *Pinus* may be attributable to fusion between lateral organs, but the distinct expression of *GpANTL1* in three domains with subsequent organogenesis is retained in *Gnetum* (Fig. 5A, B).

Recent molecular phylogenetic analyses have suggested that the extant angiosperms are distantly related to the extant gymnosperms

(Winter et al. 1999; Soltis et al. 2002; Burleigh and Mathews 2004).

Therefore, the leaves on the fertile shoots of extant gymnosperms may

or may not be homologous in a strict sense to those of angiosperms.

Nonetheless, the difference in expression between the *Gnetum* and

Pinus ANT homologs may provide an important analogy regarding the

evolutionary history of the angiosperm ovulate axis. Gymnosperms and

angiosperms have similar fertile axes, into which the unitegmic ovules

and leaves are incorporated; in gymnosperms, the middle and outer

envelopes (in *Gnetum*) and the ovuliferous scale (in conifers) are

modified leaves, while in angiosperms, the outer integument of the

bitegmic ovule may also be a modified leaf (Yamada et al. 2001a,b;

Doyle 2006). In light of the hypothesis that the two integuments evolved

from different organs at different times, they may have distinct origins.

ANT expression in the chalaza in *Arabidopsis* is partly similar to the

expression of *PtANTL1* in *Pinus* because no tissue without *ANT*

expression exists between the two integuments (Elliott et al. 1996;

Klucher et al. 1996; Mizukami and Fischer 2000; Fig. 4C). This suggests

that the internodal tissues between the outer and inner integuments are

extremely reduced (or could be congenitally fused into the chalaza) in angiosperms, like the ovuliferous scale and bract in conifers. This hypothesis is supported by the fact that the pattern of *ANT* expression in the chalaza is also observed for *BELL1*, which is involved in integument formation (Reiser et al. 1995; Klucher et al. 1996; Baker et al. 1997; Gasser at al. 1998; Balasubramanian and Schneitz 2000, 2002). The role which the internode played in the ovulate axis evolution could be tested by examining the involvement of genes regulating internode growth, such as BREVIPEDICELLUS/OSH15 homologs (Sato et al. 1999; Douglas et al. 2002; Venglat et al. 2002; Smith and Hake 2003), in seed plants.

Acknowledgements

REFERENCES

Abascal, F., Zardoya, R., and Posada, D. 2005. ProtTest: Selection of best-fit models of protein evolution. *Bioinformatics* 21: 2104-2105.

Baker, S. C., Robimson-Beers, K., Villanueva, J. M., Gaiser, J. C., and Gasser, C. S. 1997. Interaction among genes regulating ovule development in *Arabidopsis thaliana*. *Genetics* 145: 1109-1124.

Balasubramanian, S., and Schneitz, K. 2000. *NOZZLE* regulates proximal-distal pattern formation, cell proliferation and early sporogenesis during ovule development in *Arabidopsis thaliana*. *Development* 127: 4227-4238.

Balasubramanian, S., and Schneitz, K. 2002. *NOZZLE* links proximal-distal and adaxial-abaxial pattern formation during ovule

development in *Arabidopsis thaliana*. *Development* 129: 4291-4300.

Bouman, F. 1984. The ovule. In: B. M. Johri (ed.). *Embryology of angiosperms*. Springer-Verlag, Berlin, pp 123-157.

Burleigh, J. G., and Mathews, S. 2004. Phylogenetic signal in nucleotide data from seed plants: implications for resolving the seed plant tree of life. *Am. J. Bot.* 91: 1599-1613.

Coulter, J. M., and Chamberlain, C. J. 1917. *Morphology of gymnosperms*, 2nd Ed. The University of Chicago Press, Chicago.

Crane, P. R. 1985. Phylogenetic analysis of seed plants and the origin of angiosperms. *Ann. Mo Bot. Gard.* 72: 716-793.

Douglas, S. J., Chunk, G., Dengler, R. E., Pelecanda, L., and Riggs, C. D. 2002. *KNAT1* and *ERECTA* regulate inflorescence architecture in Arabidopsis. *Plant Cell* 14: 547-558.

Doyle, J. A. 1996. Seed plant phylogeny and the relationships of Gnetales. *Int. J. Plant Sci.* 157 (6 Suppl.): S3-S39.

Doyle, J. A. 2006. Seed ferns and the origin of angiosperms. *J. Torrey Bot. Soc.* 133: 169-209.

Doyle, J. A., and Donoghue, M. J. 1986. Seed plant phylogeny and the

origin of angiosperms: an experimental cladistic approach. *Bot. Rev.* 52: 321-431.

Doyle, J. J., and Doyle, J. L. 1987. A rapid DNA isolation procedure for small quantities of fresh leaf tissue. *Phytochem. Bull.* 19: 11-15.

Drummond, A. J, and Rambaut, A. 2005. Tracer, version 1.3. http://evolve.zoo.ox.ac.uk/software.html?id=tracer.

Drummond, A. J, and Rambaut, A. 2006. BEAST, version 1.4. http://evolve.zoo.ox.ac.uk/beast/.

Elliott, R. C., Betzner, A. S., Huttner, E., Oskes, M. P., Tucker, W. Q. J., Gerentes, D., Perez, P., and Smyth, D. R. 1996. *AINTEGUMENTA*, an *APETALA2*-like gene of *Arabidopsis* with pleiotropic roles in ovule development and floral organ growth. *Plant Cell* 8: 155-168.

Felsenstain, J. 1994. PYHLIP (Phylogenetic Inference Package) ver. 3.56. Distributed by author. Department of Genetics, University of Washington, Seattle.

Florin, R. 1951. Evolution in cordaites and conifers. *Acta Hort. Bergiani* 15: 285-388.

Floyd, K. F., and Bowman, J. L. 2007. The ancestral developmental tool

kit of land plants. *Int. J. Plant Sci.* 168: 1-35.

Gasser, C. S., Broadhvest, J., and Hauser, B. A. 1998. Genetic analysis of ovule development. *Annu. Rev. Plant Physiol. Plant Mol. Biol.* 49: 1-24.

Gifford, E. M., and Foster, A. S. 1988: *Morphology and Evolution of Vascular Plants*, 3rd Ed. Freeman, New York.

Hasebe, M. 1999. Evolution of reproductive organs in land plants. *J. Plant Res.* 112: 463-474.

Imaichi, R., Kato, M., and Okada、H. 1995. Morphology of the outer integument in three primitive angiosperm families. *Can. J. Bot*. 73: 1242-1249.

Kim, S., Soltis, P. S., Wall, K., and Soltis, D. E. 2005. Phylogeny and domain evolution in the *APETALA2*-like gene family. *Mol. Biol. Evol.* 23: 107-120.

Klucher, K. M., Chow, H., Reiser, L., and Fischer, R. L. 1996: The *AINTEGUMENTA* gene of *Arabidopsis* required for ovule and female gametophyte development is related to the floral homeotic gene *APETALA2*. *Plant Cell* 8: 137-153.

Krizek, B. A. 1999. Ectopic expression of *AINTEGUMENTA* in *Arabidopsis* plants results in increased growth of floral organs. *Dev. Genet.* 25: 224-236.

Meister, R. J., Kotow, L. M., and Gasser, C. S. 2002. *SUPERMAN* attenuates positive *INNER NO OUTER* autoregulation to maintain polar development of *Arabidopsis* ovule outer integuments. *Development* 129: 4281-4289.

Mizukami, Y., and Fischer, R. L. 2000. Plant organ size control: *AINTEGUMENTA* regulates growth and cell numbers during organogenesis. *Proc. Natl. Acad. Sci. USA* 97: 942-947.

Nole-Wilson, S., Tranby, T. L., and Krizek, B. A. 2005. *AINTEGUMENTA*-like (*AIL*) genes are expressed in young tissues and may specify meristematic or division-competent states. *Plant Mol. Biol.* 57: 613-628.

Reiser, L., Modrusan, Z. L. M., Samach, A., Ohad, N., Haughn, G. W., and Fischer, R. L. 1995. The *BELL1* gene encodes a homeodomain protein involved in pattern formation in the *Arabidopsis* ovule primordium. *Cell* 83: 735-742.

Robinson-Beers, K., Pruitt, R. E., and Gasser, C. S., 1992. Ovule

development in wild-type *Arabidopsis* and two female sterile mutants.

Plant Cell 4: 1237-1249.

Sato, Y., Sentoku, N., Miura, Y., Hirochika, H., Kitano, H., and Matsuoka,

M. 1999. Loss-of-function mutations in the rise homeobox gene

OSH15 affect the architecture of internodes resulting in dwarf plants.

EMBO J. 18: 992-1002.

Shigyo, M., and Ito, M. 2004. Analysis of gymnosperm

two-*AP2*-domain-containing genes. *Dev. Genes Evol.* 214: 105-114.

Shigyo, M., Hasebe, M., and Ito, M. 2006. Molecular evolution of the

AP2 subfamily. *Gene* 366: 256-265.

Shindo, S., Ito, M., Ueda, K., Kato, M., and Hasebe, M. 1999.

Characterization of MADS genes in the gymnosperm *Gnetum*

parvifolium and its implication on the evolution of reproductive organs

in seed plants. *Evol. Dev.* 1: 180-190.

Sieber, P., Gheyselinck, J., Gross-Hardt, R., Laux, T., Grossniklaus, U.,

and Schneitz, K. 2004. Pattern formation during early ovule

development in *Arabidopsis thaliana*. *Dev. Biol.* 273: 321-334.

Skinner, J. D., Hill, T. A., and Gasser, C. S. 2004. Regulation of ovule development. *Plant Cell* 16: S32-S45.

Smith, H. M. S., and Hake S. 2003. The interaction of two homeobox genes, *BREVIPEDICELLUS* and *PENNYWISE*, regulates internode patterning in the Arabidopsis inflorescence. *Plant Cell* 15: 1717-1727.

Soltis, D. E., Soltis, P. S., and Zanis, M. J. 2002. Phylogeny of seed plants based on evidence from eight genes. *Am. J. Bot.* 89: 1670-1681.

Stewart, W. N., and Rothwell, G. W. 1993. *Paleobotany and the evolution of plants*, 2nd Ed. Cambridge University Press, New York.

Swofford, D. 2001. PAUP* 4.0b10: phylogenetic analysis using parsimony (*and other methods). Sinauer, Sunderland, Mass.

Takaso, T., and Bouman, F. 1986. Ovule and seed ontogeny in *Gnetum gnemon* L. *Bot. Mag. Tokyo* 99: 241-266.

Thompson, J. D., Gibson, T. J., Plewniak, F., Jeanmougin, F., Higgins, D. G. 1997. The ClustalX windows interface: flexible strategies for multiple sequence alignment aided by quality analysis tools. *Nuc. Acids Res.* 24: 4876-4882.

Venglat, S. P., Dumonceaux, T., Rozwadowski, K., Parnell, L., Babic, V., Keller, W., Martienssen, R., Selvaraj, G., Datla, R. 2002. The homeobox gene *BREVIPEDICELLUS* is a key regulator of inflorescence architecture in Arabidopsis. *Proc. Natl. Acad. Sci. USA* 99: 4730-4735.

Winter, K. U., Becker, A., Münster, T., Kim, J. T., Saedler, H., and Theissen, G. 1999. MADS-box genes reveal that gnetophytes are more closely related to conifers than to flowering plants. *Proc. Natl. Acad. Sci. USA* 96: 7342-7347.

Yamada, T., Imaichi, R., and Kato, M. 2001a. Developmental morphology of ovules and seeds of Nymphaeales. *Am. J. Bot.* 88: 963-974.

Yamada, T., Tobe, H., Imaichi, R., and Kato, M. 2001b. Developmental morphology of the ovules of *Amborella trichopoda* (Amborellaceae) and *Chloranthus serratus* (Chloranthaceae). *Bot. J. Linn. Soc.* 137: 277-290.

Yamada, T., Ito, M., and Kato, M. 2003. Expression pattern of *INNER NO OUTER* homologue in *Nymphaea* (water lily family,

Nymphaeaceae). *Dev. Genes Evol.* 213: 510-513.

Figure legends

Fig. 1. Bayesian phylogenetic tree for the *ANT* genes. The numbers above and below the branches are the bootstrap values from the MP analysis (>50%), bootstrap values from the NJ analysis (>50%), and posterior probability values from the Bayesian analysis (>80%). Those branches with >90% posterior probability values are indicated by bold black lines and those with 80–90% are indicated by bold gray lines. The branches of the *ANT* and *AP2* genes are contracted. Bar = 0.1 substitution per site.

Fig. 2. Expression of *GpANTL1* in vegetative shoots (VS), leaf primordia (LP), root tips (RT), young ovules with developing inner and middle envelopes (OV1), and ovules with three developed envelopes (OV2). *GpGAPDH* was used to normalize the amount of mRNA.

Fig. 3. Expression of *GpANTL1* in the shoot apex and ovulate axis of *Gnetum parvifolium*. (A, C, E, G) antisense probe. (B, D, F, H) sense probe (negative control). (A, B) Obliquely cross sections through shoot apex. Arrow indicates the boundary between the shoot apex and leaf primordium. Scale bars = 100 µm. (C, D) Longitudinal sections of the ovulate axis with the outer envelope completely covering the ovule and middle envelope. Expression in the inner and middle envelope is indicated by arrowheads. Scale bars = 50 µm. (E, F) Longitudinal sections of the ovulate axis at a slightly later stage than that in A and B. Expression in the inner and middle envelope is indicated by arrowheads. Scale bars = 100 µm. (G, H) Longitudinal sections of the inner and middle envelopes developing on the ovulate axis. Scale bars = 50 µm. i, integument (inner envelope); l, leaf primordium; me, middle envelope; n, nucellus; oe, outer envelope; s, shoot apex.

Fig. 4. Schematic drawings of *ANT* homolog expression. Expression is

orthogonally projected onto the median longitudinal section of the ovulate axis (shaded). (A) *GpANTL1* in *Gnetum parvifolium*. (B) *PtANTL1* in *Pinus thunbergii* (from Shigyo and Ito 2004). (C) *ANT* in *Arabidopsis thaliana* (from Elliot et al. 1996). bs, bract scale; f, funiculus; i, integument (inner envelope); ii, inner integument; me, middle envelope; n, nucellus; oe, outer envelope; oi, outer integument; os, ovuliferous scale.

Fig. 5. *ANT* homolog expression in the ovulate axes of Gnetales and Coniferales and their proposed evolution. *ANT* homolog expression in extant plants (right) and their hypothetical ancestors (left) are indicated in red. Subsumed axes are indicated by dashed lines. The phylogeny is based on Soltis et al. (2002). (A) Gnetales. (B) Coniferales. bs, bract scale; i, integument (inner envelope); l, leaf; me, middle envelope; n, nucellus; oe, outer envelope; os, ovuliferous scale.

Supplementary Material

S1. The genes used in the phylogenetic analysis are shown with their
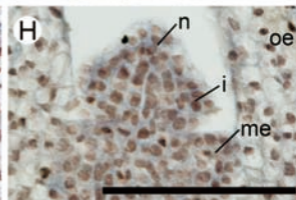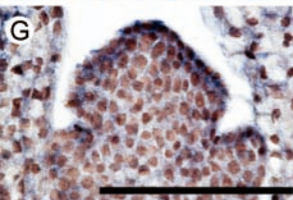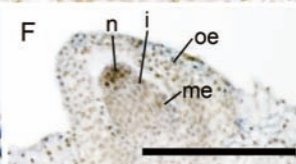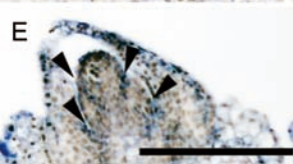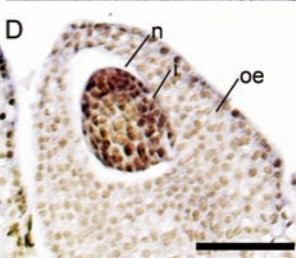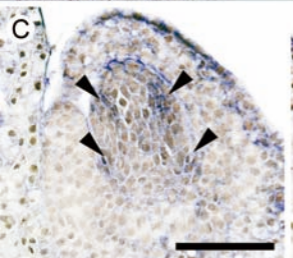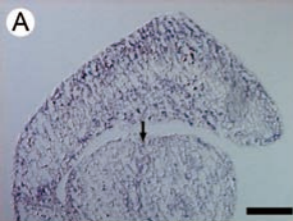
accession numbers.

Bayesian 10000000 chains
JTT+G (based on -lnL, AIC and cAIC)
MP/NJ/PP

PpANT1 *Physcomitrella patens*
86/86/99 BnBBM1 *Brassica napus*
89/93/100 BnBBM2 *Brassica napus*
69/73/99 BBM *Arabidopsis thaliana*
MtBBM *Medicago truncatula*
-/-/96 AIL5 *Arabidopsis thaliana*
GmANTL1 *Glycine max*
BAB89946 *Oryza sativa*
ZMMHCF13 *Zea mays*
NM_001056462 *Oryza sativa*
69/99/100 AIL7 *Arabidopsis thaliana*
CK267021 *Solanum tuberosum*
AIL6 *Arabidopsis thaliana*
76/87/100 EB165825 *Zea mays*
-/-/86 OSJNBb0022F16.3 *Oryza sativa*
CA783156 *Glycine max*
-/50/98 PLT1 *Arabidopsis thaliana*
70/85/99 PLT2 *Arabidopsis thaliana*

AAM191411 *Oryza sativa*
AY461432 *Nicotiana tabacum*
-/-/92 EE078047 *Vitis vinifera*
CD475882 *Nupahr advena*
AP005309 *Oryza sativa*
EE613071 *Helianthus argophyllus*
61/64/100 EL464152 *Helianthus tuberosus*
DY961435 *Lactuca sativa*
-/-/87 DQ211969 *Brassica napus*
100/100/100 ANT *Arabidopsis thaliana*
DQ211970 *Brassica napus*
59/54/98 AfpANTL1 *Aquilegia formosa x A. pubescens*
CrANTL1 *Cycas revoluta*
DR048264 *Pinus taeda*
GbANTL1 *Ginkgo biloba*
-/-/82 PtANTL1 *Pinus thunbergii*
GpANTL1 *Gnetum parvifolium*
AIL1 *Arabidopsis thaliana*

59/97/100 NM_101474 *Arabidopsis thaliana*
92/99/100 NM_106619 *Arabidopsis thaliana*
NM_001068452 *Oryza sativa*
100/100/100 WRI1 *Arabidopsis thaliana*
-/60/91 BnWRI1 *Brassica napus*
54/55/- OsANTL *Oryza sativa*
BAB85254 *Oryza sativa*

80/54/99 PtAP2L1 *Pinus thunbergii*
AP2 *Arabidopsis thaliana*
PtAP2L2 *Pinus thunbergii*
93/78/100 IDS1 *Zea mays*
AY069953 *Hordeum vulgare*

83/100/100
80/64/99
72/68/96
-/64/100
-/-/99
78/88/100
100/100/100

0.1

BBM/PLT
angioANT
gymnoANT
ANT (*sensu stricto*)
euANT
basalANT
ANT group
AP2 group

	VS	LP	RT	OV1	OV2
GpANTL1					
GpGAPDH					

Panels A–H showing labelled structures: n, i, oe, me, s, and arrowheads.

A   B   C

n   i   me   oe   os   i   n   bs   n   ii   oi   f

A

n i

n i me
oe

→ Gnetales

B

i
n

l
b

os
i n bs

→ Coniferales

Gene	Accession Number	Species
AAM191411	AC103891	*Oryza sativa*
AfpANTL1	DT750376, DT729383	*Aquilegia formosa x A. pubescens*
AIL1	DQ446422	*Arabidopsis thaliana*
AIL5	NM_125122	*Arabidopsis thaliana*
AIL6	NM_121089	*Arabidopsis thaliana*
AIL7	NM_125949	*Arabidopsis thaliana*
ANT	U40256	*Arabidopsis thaliana*
AP005309	AP005309	*Oryza sativa*
AP2	U12546	*Arabidopsis thaliana*
AY069953	AY069953	*Hordeum vulgare*
AY461432	AY461432	*Nicotiana tabacum*
BAB85254	AP003247	*Oryza sativa*
BAB89946	AP003313	*Oryza sativa*
BBM	AF317907	*Arabidopsis thaliana*
BnBBM1	AF317906	*Brassica napus*
BnBBM2	AF317905	*Brassica napus*
BnWRI1	DQ370141	*Brassica napus*
CA783156	CA783156	*Glycine max*
CD475882	CD475882	*Nuphar advena*
CK267021	CK267021	*Solanum tuberosum*
CrANTL1	AB195243	*Cycas revoluta*
DQ211969	DQ211969	*Brassica napus*
DQ211970	DQ211970	*Brassica napus*
DR048264	DR048264	*Pinus taeda*
DY961435	DY961435	*Lactuca sativa*
EB165825	EB165825	*Zea mays*
EE078047	EE078047	*Vitis vinifera*
EE613071	EE613071	*Helianthus argophyllus*
EL464152	EL464152	*Helianthus tuberosus*
GbANTL1	AB195245	*Ginkgo biloba*
GmANTL1	CF807326, AW200688	*Glycine max*
GpANTL1	AB297493	*Gnetum parvifolium*
IDS1	AF048900	*Zea mays*
MtBBM	AY899909	*Medicago truncatula*
NM_001056462	NM_001056462	*Oryza sativa*
NM_001068452	NM_001068452	*Oryza sativa*
NM_101474	NM_101474	*Arabidopsis thaliana*
NM_106619	NM_106619	*Arabidopsis thaliana*

Gene	Accession Number	Species
OsANTL	AB247626	*Oryza sativa*
OSJNBb0022F16.3	AL606446	*Oryza sativa*
PLT1	AY506549	*Arabidopsis thaliana*
PLT2	AY506550	*Arabidopsis thaliana*
PpANT1	BJ178045	*Physcomitrella patens*
PtANTL1	AB101585	*Pinus thunbergii*
PtAP2L1	AB101586	*Pinus thunbergii*
PtAP2L2	AB101587	*Pinus thunbergii*
WRI1	NM_115292	*Arabidopsis thaliana*
ZMMHCF13	Z47554	*Zea mays*